



OPEN Tribological behaviors of laser textured surface under different lubrication conditions for rotary compressor

Shaopeng Ding^{1,2}, Huijun Wei^{1,2,3}✉, Ouxiang Yang^{1,2,3}, Liying Deng^{1,2} & Di Mu²

Tribological behaviors of laser textured surface with elliptical dimples were experimentally compared with that of the smooth one under different lubrication conditions, including the poor-oil, rich-oil and dry lubrication. The lubrication regime was analyzed with the increasing operating load by ring-on-ring tribological tests. Finally, the performance impact of rolling piston rotary compressor with textures fabricated on the thrust surfaces was investigated. Results show that the tribological improvement strongly depends on lubrication condition. With the increase of applied loads under rich-oil and poor-oil lubrication, the effect of micro dimple promotes the critical load transforming lubrication regime, and expands the range of hydrodynamic lubrication, meanwhile maintains a similar minimum of friction coefficient as the smooth surface but enhances wear resistance. However, it is reverse to increase the friction coefficient and surface wear for the textured surfaces under dry lubrication. The compressor performance can be improved significantly by laser surface texturing with a 2% reduction of friction power consumption and a 2.5% enhancement of energy efficiency ratio.

Improving efficiency is an eternal topic for compressors used in air conditioners, especially with the increased awareness of global warming, and a highly efficient compressor is strongly demanded to reduce the power consumption. With the use of low global warming potential (GWP) refrigerants, the lubrication regime and operation condition in compressors will be also further worsened. The friction loss and wear failure of sliding surfaces become a main obstacle to improve performance and extend life, especially for the rolling piston rotary compressor with many sliding parts such as the sliding bearings, thrust bearing, rotating crankshaft and roller, reciprocating slide and so on.

Laser surface texturing (LST) by fabricating the regular micro-pattern on surfaces has been confirmed theoretically and practically to improve the higher load-carrying capacity and the lower friction coefficient and surface heat in hydrodynamic bearings, mechanical seals, cylindrical face rings or piston rings¹⁻⁴. This provides a substantial way to improve the tribological behaviors of friction couple.

Compared with the protective surface coating^{5,6} and structural optimization⁷ as the current main methods, the LST just artificially structures surface topography to control the lubrication regime instead of complex processing and difficult design. The micro dimples as the common textured pattern was first carried out the mechanism study of tribological benefits by theoretical modeling and experimental observation^{8,9}. It is concluded that surface micro-dimples can boost the additional hydrodynamic pressure of the convergent viscous fluid between the relative sliding components, thus expand the range of hydrodynamic lubrication. As a benefit, the micro dimples, served as micro-hydrodynamic bearings, can maintain surface separation and non-contacting operation under rich-oil condition. Besides, these micro dimples also can be acted as lubricant micro-containers to supply oil source under mixed or poor-oil lubrication, or micro-traps for wear debris to prevent further abrasive wear under dry sliding contact¹⁰.

Currently, the significant popularity on the studies of micro-dimpled textures was forced on the geometrical optimization (dimple depth¹⁰, dimple diameter¹¹, area density^{12,13}), pattern comparison (circle¹⁴, elliptical¹⁵, triangular¹⁶, diamond shape¹⁷ and flat¹⁸, spherical^{19,20}, sloped concave or convex²¹) and arrangement influence (inclination angle¹⁷, slender ratio²², distribution location²¹) with the purpose of best friction reduction and wear

¹State Key Laboratory of Air-Conditioning Equipment and System Energy Conservation, Zhuhai 519070, Guangdong, China. ²Gree Electric Appliances, Inc. of Zhuhai, Zhuhai 519070, Guangdong, China. ³Guangdong Key Laboratory of Refrigeration Equipment and Energy Conservation Technology, Zhuhai 519070, Guangdong, China. ✉email: zgddsp@126.com

resistance, especially under full-oil or rich-oil lubrication. Overall, the optimal elliptical dimples show a stronger hydrodynamic effect with a 26.3% increase of load-carrying capacity than the circle one¹⁸ due to fluid cumulative effect in the dimple length direction, and its friction coefficient can be reduced by 10–20% compared with other dimple patterns²³. So the elliptical dimples were selected and analyzed in this paper.

However, the optimal geometries with tribological benefits highly depend on operating environments²⁴ and lubrication conditions^{25,26}, which may lead to conflicting conclusions and make a difficult industrial application. For example, by pin-on-disc tests under mixed lubrication condition, Podgornik²⁵ carried out the tribological investigation on the effectiveness of surface textures to point that the textures resist sliding and increase friction in his cases with sliding speed from 0.015 to 0.45 m s⁻¹ and contact pressure of 1 MPa. But, Liew²⁷ showed the friction coefficient of dimpled surface is 11–24% lower than that of the non-textured one in his cases with sliding speed from 0.5 to 7.8 m s⁻¹ and contact pressure from 0.08 to 0.3 MPa, and Braun²⁸ also showed a friction reduction of up to 80% can be obtained for the optimal diameter at the sliding speed of 0.5 m s⁻¹ and contact pressure of 3 MPa. Though the promising results have been proved by a large number of theoretical and experimental studies, the vast majority is based on own operating condition under single lubrication mode. But for industrial applications, especially for the rolling piston rotary compressor in air conditioners, the oil supplies are ever-changing including poor-oil and even dry lubrication, and not merely rich-oil condition. This also significantly affects the lubrication regimes of friction faces from hydrodynamic to mixed or boundary lubrication. So it is lack of the comparability of dimpled optimization and influence on friction and wear properties under the same operation parameters with different lubrication conditions. So in this paper, the tribological behaviors of laser textured surface were compared experimentally under different lubrication conditions with the same operating parameters.

In compressor applications, the textured surfaces have also been paid more attention gradually due to its advantages of friction reduction and anti-wear enhancement, but the published researches still remain inadequate. Nagata²⁹ compared three textured patterns on thrust surfaces of reciprocating compressors to show that the coefficient of performance has 1.4% higher and the friction loss has 20–60% lower. Mishra³⁰ investigated the tribological behaviors of LST under poor-oil lubrication for scroll compressor within refrigeration ambient, which shows that surface texturing shows significant tribological improvements and largely independent of the type of lubricant or refrigerant. Through the influence of dimpled structures has been investigated in reciprocating or scroll compressor, its applicability and advantage on tribological properties of rotary compressor is not clear.

So, the tribological behaviors of laser textured surface with elliptical dimples were analyzed experimentally under different lubrication conditions including the poor-oil, rich-oil and dry lubrication. The friction coefficients and wear topographies were compared with the smooth one with the increasing operating load. The lubrication regime and wear mechanism were also analyzed. Finally, the performance impact of rolling piston rotary compressor with textures fabricated on the thrust surfaces was investigated.

Tribological experiments

Samples. The experimental tests were carried out on a ring-on-ring friction couple as shown in Fig. 1. The rotor, namely the upper one with the internal radius $r_i = 13.5$ mm, external radius $r_o = 20$ mm and thickness of 24 mm, was made of JIS FC300 cast iron coming from the roller of rolling piston rotary compressor. The elliptical dimples shown in Fig. 2 were processed by laser surface texturing (LST) with a certain designed depth $h_d = 5$ μ m, and its major axis was parallel to shear velocity direction. Two extra geometrical parameters were defined to describe the distribution characteristic of elliptical dimple, including the dimple area density, $S_p = n_d n_a ab / (r_o^2 - r_i^2)$, representing the percentage of the summation of dimpled area to lubrication area, and the slender ratio, $\lambda = a/b$, representing the ratio between the major radius and minor radius. The detailed meaning and dimension of each variable was listed in Table 1.

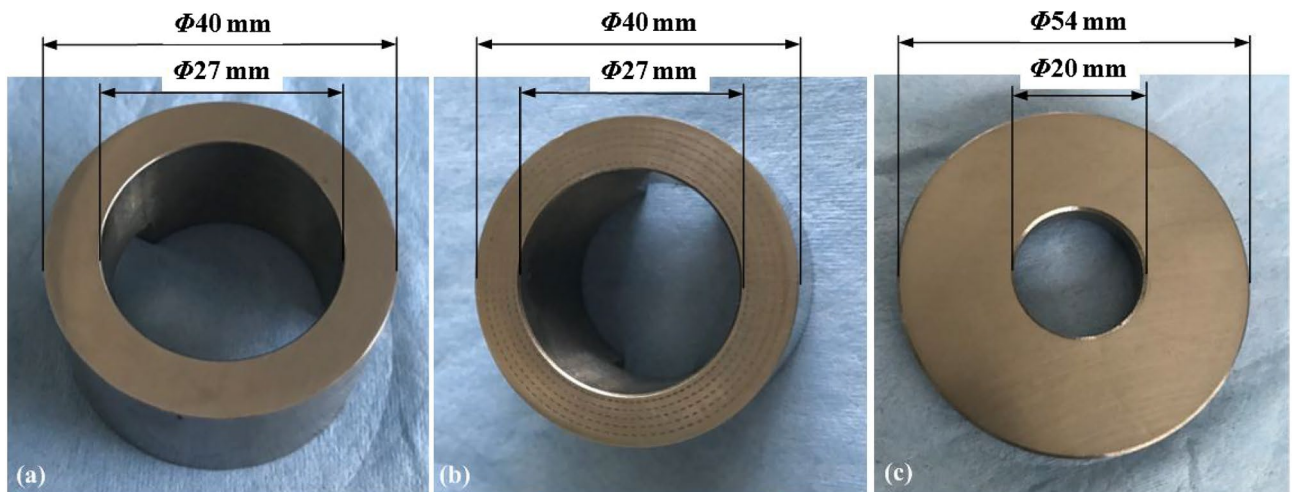


Figure 1. Photographs and dimensions of test samples: (a) rotational sample without textures; (b) rotational sample with textures; (c) stationary sample.

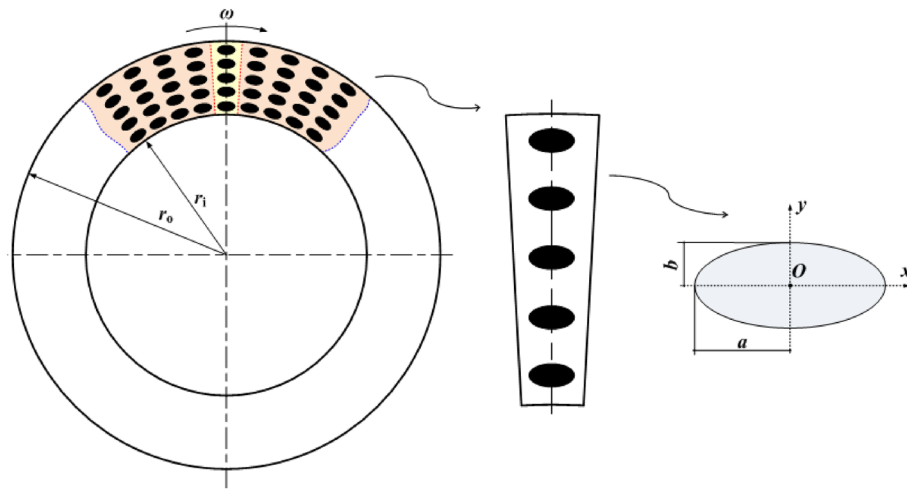


Figure 2. Geometry of textured surface with elliptical dimples.

No	Designed depth $h_d/\mu\text{m}$	Slender ratio λ	Dimple area density S_p	Dimple numbers		Dimple patterns
				Circumferential direction n_θ	Radial direction n_r	
1#	–	–	–	–	–	Smooth
2#	5.0	2	9.5%	100	5	Ellipse

Table 1. Meanings and dimensions of different geometrical parameters of elliptical dimples on rotor surfaces.

Before laser processing, the original rotor surface was polished with the roughness about $Ra < 0.2 \mu\text{m}$, then was cleaned in an ultrasonic cleaner with acetone and alcohol, and dried in oven. The micro-dimpled textures were fabricated by fiber optical laser from HGTECH LSF20 with a wavelength 1064 nm. The processing parameters contained the laser power of 7 W, scanning speed of 800 mm s^{-1} , frequency of 80 kHz and 3 overscan. After fabricating by fiber optical laser, the polishing process was repeated to remove ridges or bulges around the dimples owing to metal melting by thermal diffusion. The roughness on non-textured surface was controlled in $Ra < 0.2$. The topographies were measured by a white-light interfering 3D profilometer supported by BRUKER Contour GT-K shown in Fig. 3. The measured depth was $4.61 \mu\text{m}$ instead of the designed value of $5 \mu\text{m}$.

The stator, namely the bottom one with the internal radius of 10 mm, external radius of 27 mm and thickness of 7 mm, was made of HT250 cast iron, a common bearing material in rolling piston rotary compressor. The stator surface was also polished with the roughness about $Ra < 0.2 \mu\text{m}$.

Testing parameters. Tribological behaviors of the laser textured specimens were compared with the smooth one under different lubrication conditions and operating loads by a MMW-1A tribometer. The test rig was shown in Fig. 4 with the ring-on-ring mates under ambient pressure. The upper textured rotor was driven by a rotating motor with a certain rotational speed of 1500 r min^{-1} . The bottom smooth stator was clamped in the fixed support, and sustained the vertical applied load. Table 2 lists the operating conditions. Each group test was conducted for 60 min, and was repeated at least three times. The friction torque and friction coefficient were measured. While the testing was completed, the wear topographies on frictional surfaces were presented by SEM analysis (FEI Quanta 250).

The influences of different lubrication conditions on tribological performances were compared including the poor-oil, rich-oil and dry lubrication. To the rich-oil lubrication, during the whole running, the rotor and stator were submerged into the lubricant (FV50S) with a certain volume of 100 mL. To the poor-oil one, the lubricant was evenly applied to the friction interface before startup, but there was no subsequently lubricant supplying. To the dry lubrication, any lubricant was not been provided.

Friction and wear characteristics. In the author's last article²³, the tribological behaviors under rich-oil condition have been analyzed. Figure 5 compares the friction coefficients of textured surface with the smooth one under rich-oil and poor-oil lubrication conditions with the increase of time and loads. It should be noted that each load condition represents a separate test, and then these obtained results are combined together into one figure. Each test with new specimens and lubricant is conducted from 0 to 60 min.

Generally speaking, to any case with the certain applied load, as the running time increases, the friction coefficient firstly increases rapidly during the start-up and acceleration phases from $\omega = 0$ to 1500 r min^{-1} , then decreases slowly while entering into the stable wear stage, finally maintains steady approximately. However, this

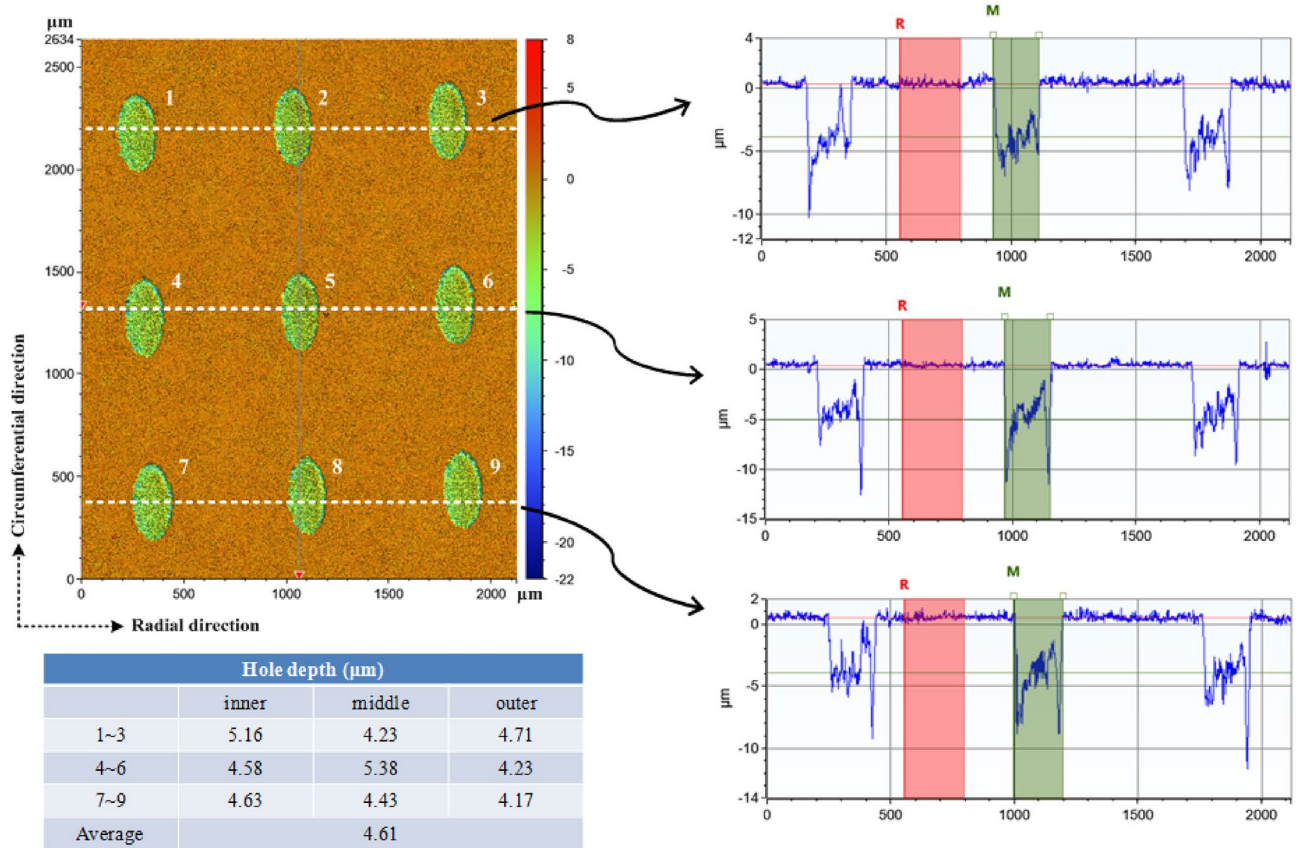


Figure 3. Topographies of the elliptical dimpled surface.

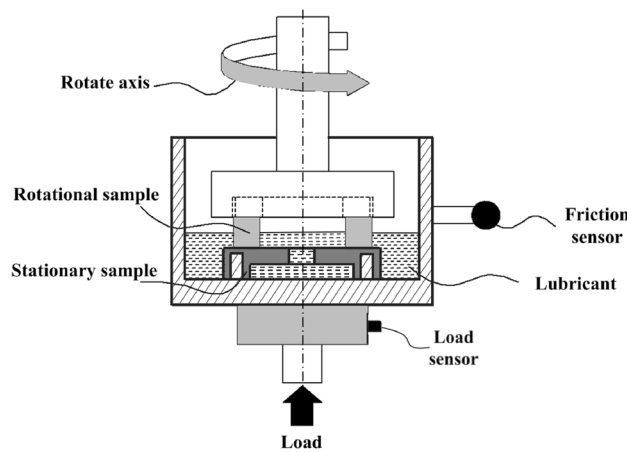


Figure 4. Schematic of test rig.

has several special operating condition such as $F = 700\text{ N}$ for the smooth surface under rich-oil lubrication and $600\text{--}700\text{ N}$ for the textured one under poor-oil lubrication. The friction coefficient f increases sharply before entering into the stable wear stage. Here, the friction interface occurs serious wear. Besides, to $F = 600\text{--}700\text{ N}$ for the smooth surface under poor-oil lubrication, the f breaks the steady value and increases sharply along with significant vibration, indicating surface wear failure. As a result, the test is forced to end without running for 60 min.

With the load increasing from 100 to 700 N, to the textured surface with elliptical dimples, the friction coefficient presents a decreasing tendency under rich-oil lubrication. It is similar under poor-oil lubrication when $F < 400\text{ N}$, but the difference is that a minimum emerges at $F = 400\text{--}500\text{ N}$, then f increases with a larger amplitude. To the smooth surface, the lubrication conditions generate slight impact on the curve of f , just change the value instead of the tendency. As similar as the textured surface under poor-oil lubrication, their minimums are at about 300–400 N.

Item	Symbol	Dimensions and data
Pressure in inner diameter	P_{in}	101,325 Pa
Pressure in outer diameter	P_{out}	101,325 Pa
Rotational speed	ω	1500 r min ⁻¹
Applied load	F	100–700 N
Lubrication condition	–	Poor-oil lubrication
		Rich-oil lubrication
		Dry lubrication

Table 2. Operating conditions during tests.

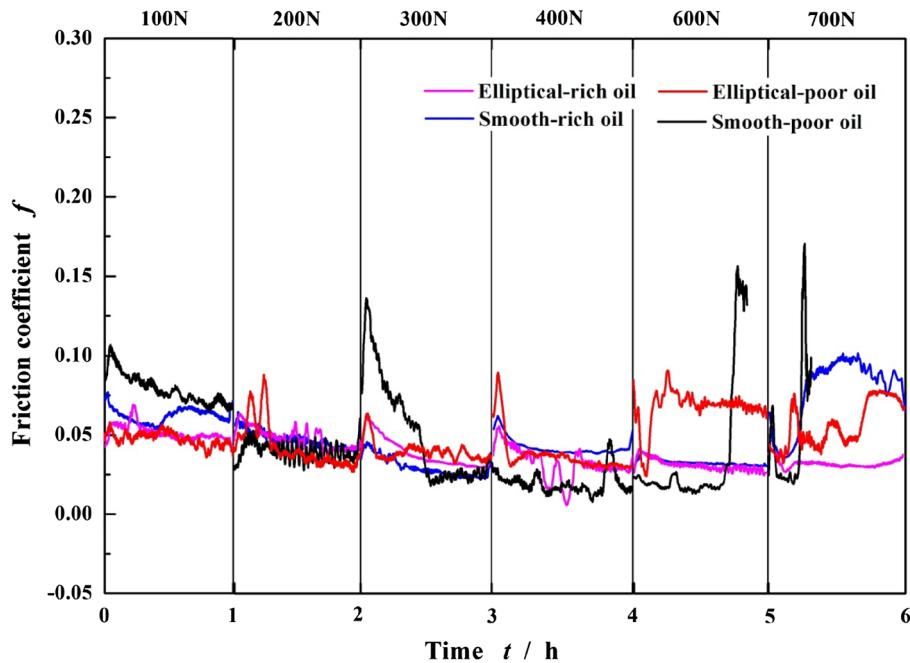


Figure 5. Friction coefficients of smooth surface and elliptical dimpled surface with the increase of time and loads under rich and poor lubrication conditions.

The friction coefficients of steady phase (in Fig. 5) for the textured and smooth specimens under different applied loads and lubrication conditions are analyzed to form the Stribeck curves shown in Fig. 6. The dimensionless parameter $\eta\omega/p$ acts as the abscissa, the friction coefficient f acts as the ordinate. As the $\eta\omega/p$ decreases (right-to-left viewing), namely the applied load increases while η and ω keep constant, for the smooth surface under two lubrication conditions, the changes of f are pretty close. Results show that the f firstly decreases and reaches a minimum at $F=300$ N, 0.025 for rich-oil lubrication and 0.029 for poor-oil lubrication respectively, then increases with a larger amplitude. This phenomenon illustrates the lubrication regime transforms from hydrodynamic into mixed lubrication near $F=300$ N. When $F<300$ N, the smooth surface is in hydrodynamic lubrication in which the poor-oil condition presents a smaller friction coefficient than the rich-oil one. Conversely, when $F>300$ N under mixed regime, the rich-oil condition shows the better friction reduction advantages.

While the tests were completed, the wear topographies on frictional surfaces of bottom specimens were presented by SEM analysis under oil film lubrication conditions as shown in Fig. 7. To the surface versus the smooth upper specimen, a similar development trend of wear topographies can be found clearly. The surfaces distribute the widely original machining scars and cracks in $F=100$ N, and the slight wear scars in $F=200$ N. With the load increasing to 300 N, the ploughing scars induced by two-body abrasive wear and plastic extrusions induced by three-body abrasive wear are formed gradually. Besides, the partial adhesive particles and pits also can be existed under poor-oil condition. When the F reached beyond 500 N, the material loss owing to the deep ploughing scars and serious plastic extrusion becomes the main wear mode. Overall, When $F<300$ N under hydrodynamic lubrication analyzed in Fig. 6, the poor-oil condition presents a similar wear resistance as the rich-oil one, and the abrasive wear is the dominant wear mechanism. When $F>300$ N under mixed regime, the material loss induced by mechanical rubbing between the rotor and stator is the dominant wear mechanism, and the rich-oil condition presents a better wear resistance.

To summarize the smooth surface, when the friction interface is in hydrodynamic lubrication regime, it is not that the more lubricant, the better friction behavior. It just needs a certain amount of lubricant to ensure the

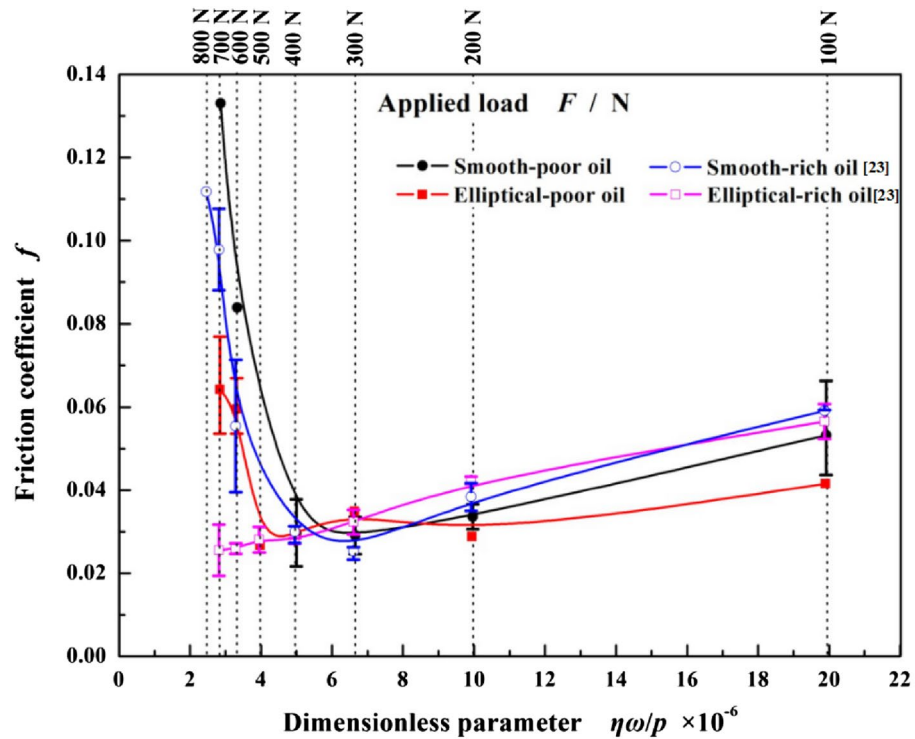


Figure 6. Friction coefficients of smooth and elliptical dimpled surfaces with the increase of dimensionless parameter under rich²³ and poor lubrication conditions (η is the viscosity of the lubricant, p , the load per unit area and ω , the rotational speed).

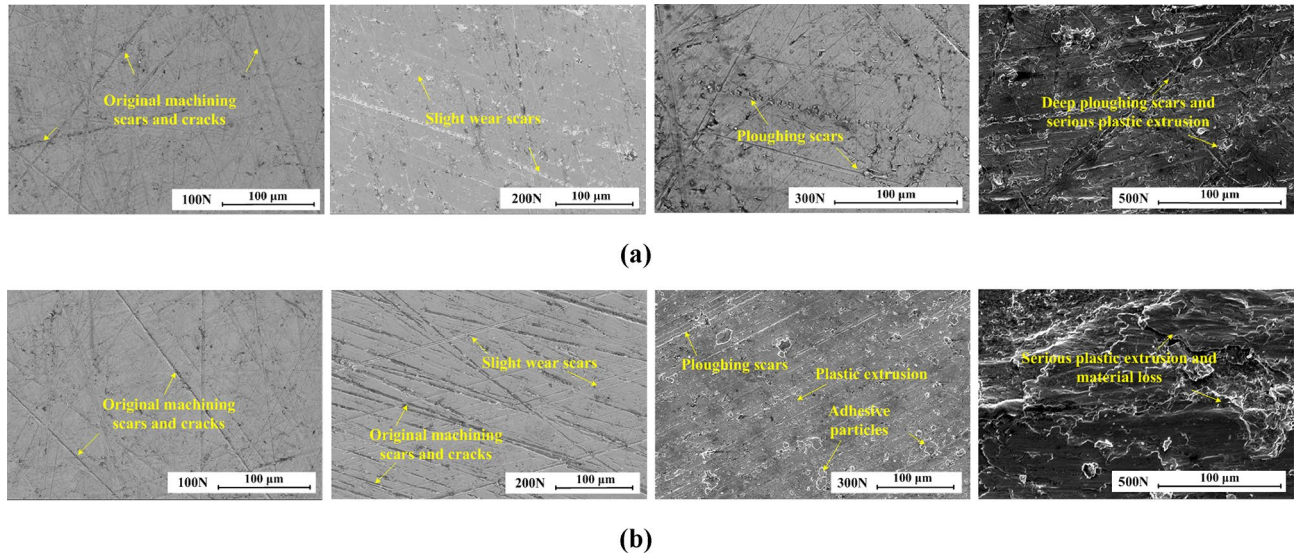


Figure 7. Wear topographies of bottom specimens versus the smooth upper specimens: (a) under rich-oil lubrication condition; (b) under poor-oil lubrication condition.

continuous oil film. Here, this can obtain the lower friction power consumption, meanwhile maintain similar wear resistance as the rich-oil condition. But when in mixed lubrication regime, the more lubricant can guarantee the better friction reduce and wear resistance.

For the textured surface under poor-oil condition in Fig. 6, the f presents a similar tendency to that of smooth one. The dimples improve the critical load from 300 N for smooth surfaces to 400–500 N, thus extend the range of hydrodynamic regime, which contributes to enhance the tribological performance. And the minimum is about 0.030 closed to the smooth one. But for the rich-oil condition, the f decreases invariably with the increase of

applied load and has no inflexion, which illustrates the textured surface always maintains hydrodynamic lubrication regime. To this, the reason may be attributed to that a significant hydrodynamic effect induced by elliptical dimples enhances the load carrying capacity of oil film to establish the steady hydrodynamic lubrication. Another is that the dimples can be served as a micro-reservoir to supply sustained lubrication under applied load^{30–33}.

Figure 8 shows the wear topographies of bottom specimens versus the textured upper specimens. Under rich-oil condition, the only slight wear scars and the original machining scars or cracks are presented. However, under poor-oil condition, the original machining features are disappeared after running the stable wear stage, as a result, the frictional interfaces become much smoother. When $F > 400$ N under mixed regime analyzed in Fig. 6, the slight ploughing scars and plastic extrusions are formed gradually. Compared with the smooth one, under the hydrodynamic regime, the laser surface texturing does not generate influences on wear resistance, but under the mixed regime, the wear resistance can be obtained significant improvement. The reason for this is that the dimples served as lubricant container to provide sufficient lubrication condition for the mating surfaces. While applying load, the micro dimples can maintain the stable oil film. The hydrodynamic effect enhances the load carrying capacity of oil film, thus makes the mating surfaces separate and keeps the non-contact running³⁴.

In conclusion, compared with the smooth surface without textures under oil film lubrication, the textured surfaces with elliptical dimples can effectively improve the lubrication regime and enhance wear resistance, especially for rich-oil condition and high applied load because of the more significant hydrodynamic effect of elliptical dimples. In present case, the friction coefficient decreases significant when the applied load is greater than 500 N under rich-oil condition.

Figure 9 shows the curves of friction coefficient of textured surface and smooth surface under dry lubrication conditions. When the applied load is controlled in 100–700 N, the friction interface fails sharply shortly with test start-up. So the load of 10–50 N is applied in present dry lubrication. It is found that the friction coefficient f significantly increases compared with the oil film lubrication, and the maximum can reach about 1.5. Besides, the f of textured surface is greater than that of the smooth one, which shows the dimpled textures have no the advantage of friction reduction and make the opposite effect. So the laser surface texturing is not recommended in dry lubrication condition if with the purpose of improving tribological behavior.

Wear topographies under dry lubrication condition in Fig. 10 can be found that the frictional interface generates the serious oxidation wear by EDS analysis, and the wear severity is similar for the textured and smooth specimens. The oxides are easy to be peeled off under the large localized contact pressure due to the plastic extrusion by mechanical contact by SEM analysis.

Compressor performance tests

By the above analysis, the surface textures can effectively decrease friction coefficient and enhance wear resistance especially for rich-oil condition and high applied load²⁶. So the laser surface texturing is extremely suitable for the thrust bearing as shown in Fig. 11 to reduce the friction power consumption and improve the energy efficiency ratio.

Figure 11 gives the schematic of rolling piston rotary compressor with two cylinders used to test. The contact interface between the bottom bearing and crankshaft is known as the thrust surface as shown in Fig. 12. On the surface of bottom bearing, the textures with ellipses are distributed with the same parameters as Table 1. The photographs of textured surfaces are shown in Fig. 13. Referring to two test plans, the distribution range of elliptical textures in 'Plan 1' is from $\Phi 18.007$ to $\Phi 33$ mm, and 'Plan 2', from $\Phi 18.007$ to $\Phi 27$ mm. Test conditions are listed on Table 3.

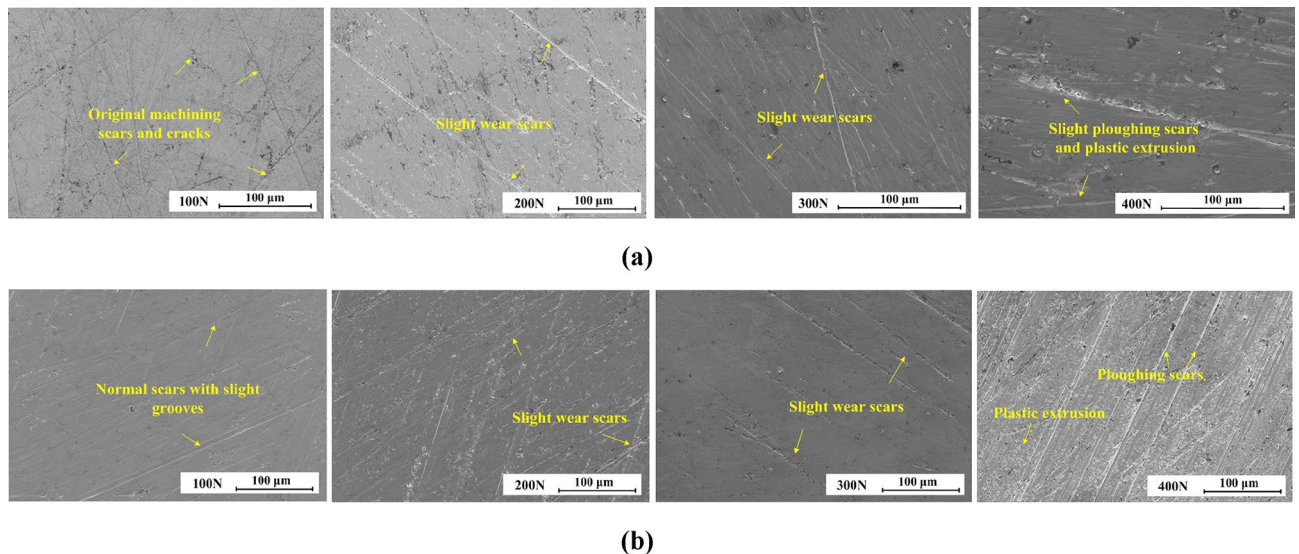


Figure 8. Wear topographies of bottom specimens versus the textured upper specimens: (a) under rich-oil lubrication condition; (b) under poor-oil lubrication condition.

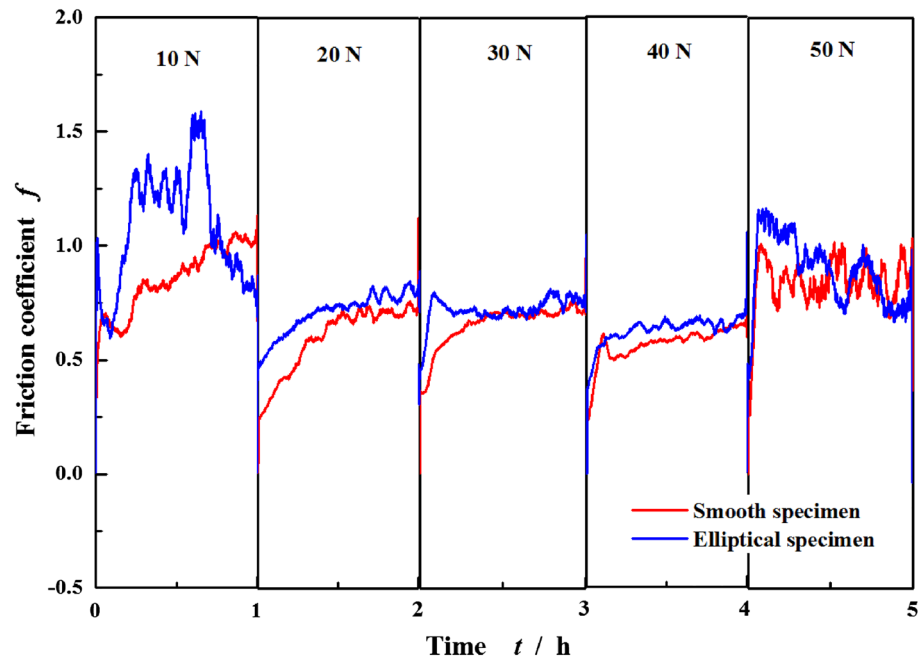


Figure 9. Friction coefficients of smooth surface and elliptical dimpled surface with the increase of time and loads under dry lubrication conditions.

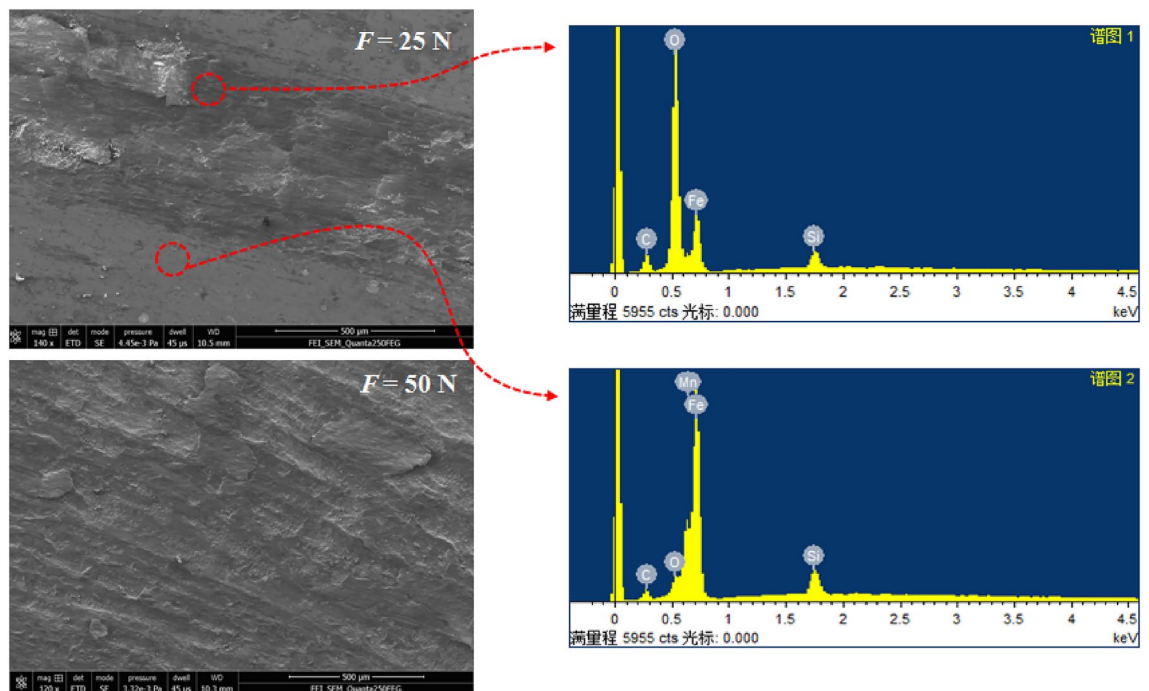


Figure 10. Wear topographies under dry lubrication condition.

The compressor test was conducted in Gree Electric Appliances, Inc. of Zhuhai (Guangdong Zhuhai, China) with the compressor performance test bench supported by Shanghai Tianhan Air-handling Equipment Co., Ltd. Performance parameters including the cooling capacity, input power, COP (= cool capacity/input power) and current for compressor with fixed frequency can be obtained.

A large number of compressor samples were tested to get this average performance value and weaken the influence of the measurement error. Three identical compressors for each plan with textures were tested with a comparison of original plan without textures. The test data was listed in Table 4. During testing process, the consistency of testing environment and the continuity of testing time were ensured. Results in Fig. 14 show that textures fabricated on the thrust surfaces can significantly decrease the power input of compressor with the 1.8%

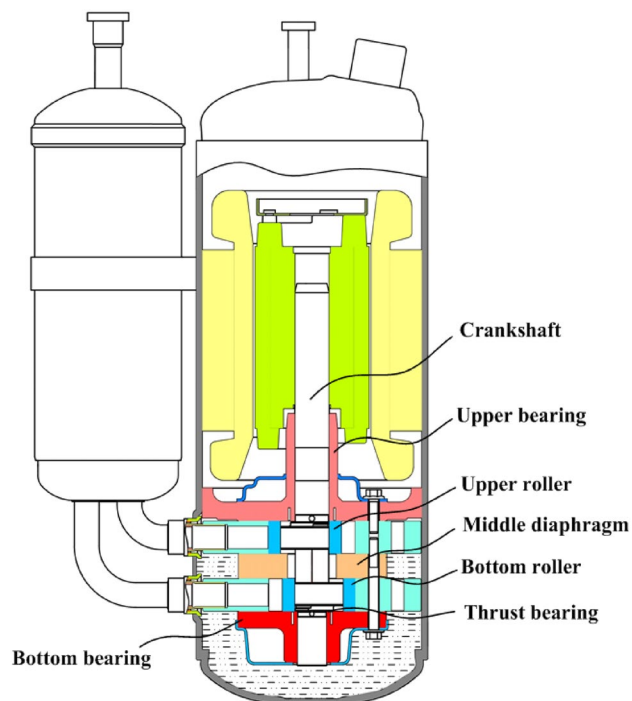


Figure 11. Schematic of test compressor.

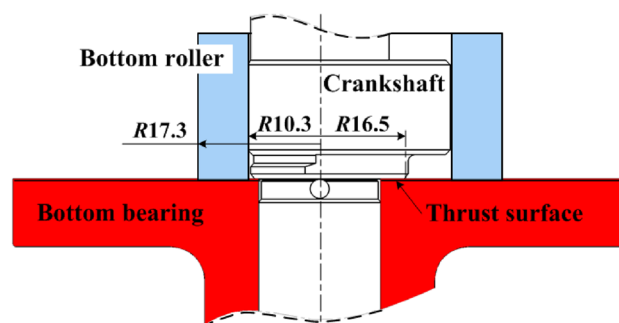


Figure 12. Thrust surface.

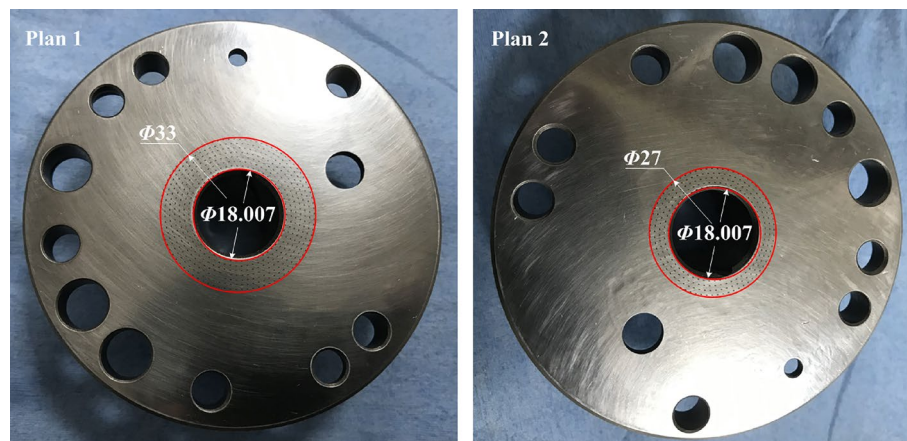


Figure 13. Photographs of bottom bearing with textures.

Item	Dimensions and data
Condensing temperature	65 °C
Evaporating temperature	13 °C
Subcooling degree	7 °C
Suction temperature	24 °C
Ambient temperature	35 °C
Frequency	60 Hz

Table 3. Compressor operating conditions.

Test schemes	Compressor number	Cooling capacity/W	Input power/W	COP
Original plan without textures	NO. 01	7852.7	3770.9	2.08
	NO. 02	8016.3	3756.6	2.13
	NO. 03	7933.5	3768.8	2.11
	Average value	7934.2	3765.4	2.11
Plan 1# with textures	NO. 04	7871.8	3702.9	2.13
	NO. 05	8034.2	3683.8	2.18
	NO. 06	7990.5	3700.9	2.16
	Average value	7965.5	3695.9	2.16
Plan 2# with textures	NO. 07	8087.7	3682.7	2.20
	NO. 08	7946.6	3663.7	2.17
	NO. 09	7814.1	3700.9	2.11
	Average value	7949.5	3682.4	2.16

Table 4. Compressor performance test data.

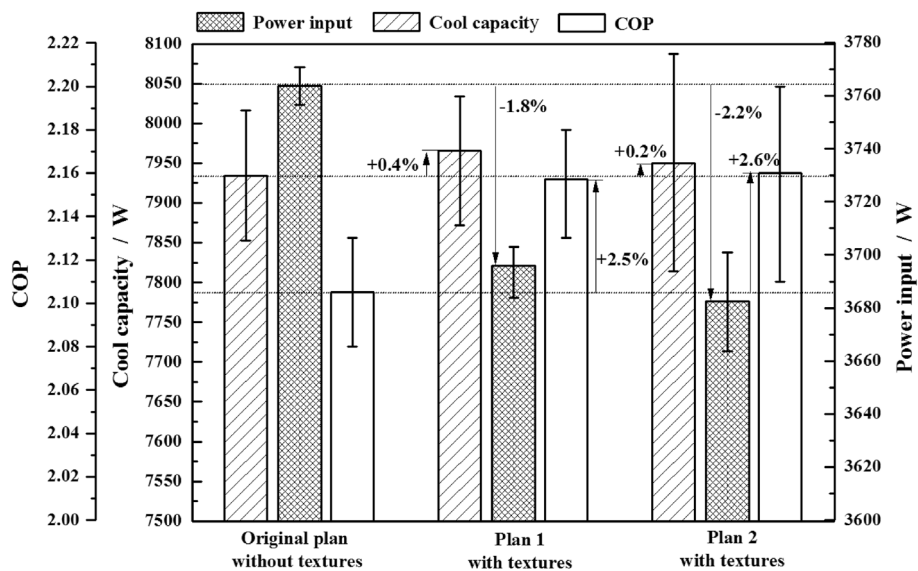


Figure 14. Comparisons of compressor performance for different plans.

reduction in Plan 1 and 2.2% in Plan 2. Meanwhile it has no influence on the cool capacity, which performs just 0.4% and 0.2% increase. As a result, the coefficient of performance (COP) can enhance 2.5% and 2.6% for Plan 1 and Plan 2 respectively. Besides, the two textured plans are effective to reduce the friction power consumption and improve the energy efficiency ratio, and have no obvious differences between them.

Conclusions

The tribological benefits of laser textures were experimentally compared under different lubrication conditions by tribological tests, and verified by thrust surface for rolling piston rotary compressors. The lubrication regime and wear mechanism were discussed by friction coefficients and wear topographies. The following conclusions were drawn.

- (1) The tribological improvement by textured surfaces strongly depends on lubrication condition. With the increase of applied loads under rich-oil and poor-oil lubrications, the effect of micro dimple promotes the critical load transforming lubrication regime, and expands the range of hydrodynamic lubrication, meanwhile maintains a similar minimum of friction coefficient as the smooth surface but enhances wear resistance. However, it is reverse to increase the friction coefficient for the textured surfaces under dry lubrication.
- (2) The surface textures can effectively decrease friction coefficient and enhance wear resistance especially for rich-oil condition and high applied load because of the more significant hydrodynamic effect of elliptical dimples. But it is not recommended in dry lubrication condition if with the purpose of improving tribological behavior. The abrasive wear is the dominant wear mechanism under oil film lubrication, but oxidation wear under dry lubrication.
- (3) The compressor performance can be improved significantly by laser surface texturing, which is effective to reduce the friction power consumption and improve the energy efficiency ratio, and have no obvious influences on the cool capacity. In present cases, the power input of compressor can be decreased ~ 2%, and the coefficient of performance (COP) can enhance ~ 2.5%.

Data availability

All data generated or analyzed during this study are included in this published article.

Received: 15 February 2023; Accepted: 28 March 2023

Published online: 03 April 2023

References

1. Wang, X. L., Kato, K. & Adachi, K. Loads carrying capacity map for the surface texture design of SiC thrust bearing sliding in water. *Tribol. Int.* **36**(3), 189–197 (2003).
2. Kovalchenko, A., Ajayi, O., Erdemir, A. & Fenske, G. Friction and wear behavior of laser textured surface under lubricated initial point contact. *Wear* **271**(9–10), 1719–1725 (2011).
3. Meng, Y. G., Xu, J., Jin, Z. M., Prakash, B. & Hu, Y. Z. A review of recent advances in tribology. *Friction* **8**, 221–300 (2020).
4. Ryk, G. & Etsion, I. Testing piston rings with partial laser surface texturing for friction reduction. *Wear* **261**(7–8), 792–796 (2006).
5. De Mello, J. D. B., Binder, R., Demas, N. G. & Polycarpou, A. A. Effect of the actual environment present in hermetic compressors on the tribological behavior of a Si-rich multifunctional DLC coating. *Wear* **267**, 907–915 (2009).
6. Solzak, T. A. & Polycarpou, A. A. Tribology of WC/C coatings for use in oil-less piston-type compressors. *Surf. Coat. Tech.* **201**(7), 4260–4265 (2006).
7. Liu, Y. G., Hung, C. H. & Chang, Y. C. Design optimization of scroll compressor applied for frictional losses evaluation. *Int. J. Refrig.* **33**(3), 615–624 (2010).
8. Etsion, I. & Burstein, L. A model for mechanical seals with regular microsurface structure. *Tribol. Trans.* **39**(3), 677–683 (1996).
9. Etsion, I. & Halperin, G. A laser surface textured hydrostatic mechanical seals. *Tribol. Trans.* **45**(3), 430–434 (2002).
10. Yu, H. W., Huang, W. & Wang, X. L. Dimple patterns design for different circumstances. *Lubric. Sci.* **25**(2), 67–78 (2013).
11. Bhaumik, S. *et al.* Analysing the frictional properties of micro dimpled surface created by milling machine under lubricated condition. *Tribol. Int.* **146**, 106260 (2020).
12. Koszela, W., Dzierwa, A. & Galda, L. Experimental investigation of oil pockets effect on abrasive wear resistance. *Tribol. Int.* **46**(1), 145–153 (2012).
13. Galda, L., Pawlus, P. & Sep, J. Dimples shape and distribution effect on characteristics of Stribeck curve. *Tribol. Int.* **42**(10), 1505–1512 (2009).
14. Andersson, P. *et al.* Microlubrication effect by laser-textured steel surfaces. *Wear* **262**(3–4), 369–379 (2007).
15. Bai, L. Q. & Bai, S. X. Frictional performance of a textured surface with elliptical dimples: Geometric and distribution effects. *Tribol. Trans.* **57**(6), 1122–1128 (2014).
16. Lu, P., Wood, R., Gee, M., Wang, L. & Pflöging, W. A novel surface texture shape for directional friction control. *Tribol. Lett.* **66**(1), 51 (2018).
17. Meng, X. K., Bai, S. X. & Peng, X. D. Lubrication film flow control by oriented dimples for liquid lubricated mechanical seals. *Tribol. Int.* **77**, 132–141 (2014).
18. Yu, H. W., Wang, X. L. & Zhou, F. Geometric shape effects of surface texture on the generation of hydrodynamic pressure between conformal contacting surfaces. *Tribol. Lett.* **37**(2), 123–130 (2010).
19. Hu, D., Guo, Z. W., Xie, X. & Yuan, C. Q. Effect of spherical-convex surface texture on tribological performance of water-lubricated bearing. *Tribol. Int.* **134**, 341–351 (2019).
20. Yang, X. P., Fu, Y. H., Ji, J. H., Chen, T. Y. & Pan, C. Y. Study on tribological properties of surface concave convex micro-texture on the mold steel. *Ind. Lubr. Tribol.* **72**(10), 1167–1171 (2020).
21. Tala-Ighil, N., Fillon, M. & Maspeyrot, P. Effect of textured area on the performances of a hydrodynamic journal bearing. *Tribol. Int.* **44**(3), 211–219 (2011).
22. Bai, S. X., Peng, X. D., Li, J. Y. & Meng, X. K. Experimental study on hydrodynamic effect of orientation micro-pored surfaces. *Sci. China Tech. Sci.* **54**(3), 659–662 (2011).
23. Ding, S. P. *et al.* Geometric influence on friction and wear performance of cast iron with a micro-dimpled surface. *Results Eng.* **9**, 100211 (2021).
24. Gropper, D., Wang, L. & Harvey, T. J. Hydrodynamic lubrication of textured surfaces: A review of modeling techniques and key findings. *Tribol. Int.* **94**(1), 509–529 (2016).
25. Podgornik, B., Vilhena, L. M., Sedlacek, M., Rek, Z. & Zun, I. Effectiveness and design of surface texturing for different lubrication regimes. *Meccanica* **47**(7), 1613–1622 (2012).

26. Kovalchenko, A., Ajayi, O., Erdemir, A., Fenske, G. & Etsion, I. The effect of laser surface texturing on transitions in lubrication regimes during unidirectional sliding contact. *Tribol. Int.* **38**(3), 219–225 (2005).
27. Liew, K. W., Kok, C. K. & Ervina, M. N. Effect of EDM dimple geometry on friction reduction under boundary and mixed lubrication. *Tribol. Int.* **101**, 1–9 (2016).
28. Braun, D., Greiner, C., Schneider, J. & Gumbsch, P. Efficiency of laser surface texturing in the reduction of friction under mixed lubrication. *Tribol. Int.* **77**, 142–147 (2014).
29. Nagata, S., Kohsokabe, H. & Sekiyama, N. A low friction thrust bearing for reciprocating compressors. In *International Compressor Engineering Conference at Purdue* (2012).
30. Mishra, S. P. & Polycarpou, A. A. Tribological studies of unpolished laser surface textures under starved lubrication conditions for use in air-conditioning and refrigeration compressors. *Tribol. Int.* **44**(12), 1890–1901 (2011).
31. Ji, J. H., Guan, C. W. & Fu, Y. H. Effect of micro-dimples on hydrodynamic lubrication of textured sinusoidal roughness surfaces. *Chin. J. Mech. Eng.* **31**(4), 160–167 (2018).
32. Ge, D. L. *et al.* Effect of micro-textures on cutting fluid lubrication of cemented carbide tools. *Int. J. Adv. Manuf. Tech.* **103**, 3887–3899 (2019).
33. Ge, D. L. *et al.* Effect of surface wettability on tribological properties of Al₂O₃/TiC ceramic under wet lubrication. *Ceram. Int.* **45**(18), 24554–24563 (2019).
34. Hu, S., Zheng, L., Guo, Q. G. & Ren, L. Q. Influence of cross-grooved texture shape on tribological performance under mixed lubrication. *Coatings* **12**(3), 305 (2022).

Acknowledgements

The research was financially supported by the Guangdong Basic and Applied Basic Research Foundation (No. 2020A1515011386).

Author contributions

All authors contributed to the study conception and design. Material preparation, experimental test and data analysis were performed by S.D., H.W., D.M. and L.D. The first draft of the manuscript was written by S.D. O.Y. and H.W. reviewed and edited the manuscript. S.D. was responsible for the funding acquisition. All authors read and approved the final manuscript.

Competing interests

The authors declare no competing interests.

Additional information

Correspondence and requests for materials should be addressed to H.W.

Reprints and permissions information is available at www.nature.com/reprints.

Publisher's note Springer Nature remains neutral with regard to jurisdictional claims in published maps and institutional affiliations.



Open Access This article is licensed under a Creative Commons Attribution 4.0 International License, which permits use, sharing, adaptation, distribution and reproduction in any medium or format, as long as you give appropriate credit to the original author(s) and the source, provide a link to the Creative Commons licence, and indicate if changes were made. The images or other third party material in this article are included in the article's Creative Commons licence, unless indicated otherwise in a credit line to the material. If material is not included in the article's Creative Commons licence and your intended use is not permitted by statutory regulation or exceeds the permitted use, you will need to obtain permission directly from the copyright holder. To view a copy of this licence, visit <http://creativecommons.org/licenses/by/4.0/>.

© The Author(s) 2023